Inorg. Chem. **2008**, *47*, 8985−8989

Flux Synthesis, Crystal Structures, and Luminescence Properties of Salt-Inclusion Lanthanide Silicates: $[K_9F_2][Ln_3Si_{12}O_{32}]$ (Ln = Sm, Eu, Gd)

Ming-Feng Tang,[†] Pei-Yun Chiang,[†] Yu-Han Su,[†] Yu-Chi Jung,[†] Guang-Yi Hou,[†] Bor-Chen Chang,[†] and Kwang-Hwa Lii*[,†,‡]

Department of Chemistry, National Central University, Jhongli, Taiwan, R.O.C., and Institute of Chemistry, Academia Sinica, Taipei, Taiwan, R.O.C.

Received June 1, 2008

New salt-inclusion lanthanide silicates, $[K_9F_2][Ln_3Si_{12}O_{32}]$ (Ln = Sm, Eu, Gd), have been synthesized using a KF-MoO_3 flux, and structurally characterized by single-crystal and powder X-ray diffraction. The structures of these three isostructural compounds consist of open-branched fünfer silicate single layers with six-, eight-, and twelve-membered rings, which are connected via LnO_6 octahedra to form a 3-D framework. The F^- and K^+ ions are located in the structural channels and form a F_2K_7 dimer with a structure similar to that of Cl_2O_7. The photoluminescence properties of the Eu compound have also been studied. The sharp peaks in the room-temperature emission spectrum are assigned and the relative intensities of the $^5D_0 \rightarrow {}^7F_1$ and $^5D_0 \rightarrow {}^7F_2$ transitions are consistent with the crystallography results. Crystal data for the Eu compound: triclinic, space group $P\bar{1}$ (No. 2), $a = 6.8989(2)$ Å, $b = 11.3834(4)$ Å, $c = 11.4955(4)$ Å, $\alpha = 87.620(2)°$, $\beta = 89.532(2)°$, $\gamma = 80.221(2)°$, and $Z = 2$. Crystal data for the Sm compound: The same as those for the Eu compound except $a = 6.9152(6)$ Å, $b = 11.400(1)$ Å, $c = 11.531(1)$ Å, $\alpha = 87.610(1)°$, $\beta = 89.445(1)°$, and $\gamma = 80.081(1)°$.

Introduction

Salt-inclusion compounds form an interesting class of host−guest materials, wherein structures of ionic compounds are incorporated in host lattices. Recently, we reported flux synthesis of a salt-inclusion stannosilicate, $[Na_3F][SnSi_3O_9]$.[1] The F^- and Na^+ ions are located in the structural channels and form a dimer with the *anti*-Al_2Cl_6(g) structure. This stannosilicate adopts a new structure and is the first metal silicate that contains both F^- and Na^+ ions in the channels. Schmidt and Glaum synthesized a series of chromous disilicates with the composition of $Cr_3Si_2O_7 \cdot {}^1/_4MX$ (MX = NaCl, NaBr, KCl, KBr).[2] The alkali-metal cations and halide anions are located in different cages in the structure. Several salt-containing manganese and iron silicates with polar framework structures were reported by Hwu and co-workers.[3,4] Their work demonstrates the utility of salt-inclusion in the synthesis of noncentrosymmetric frameworks. The interesting framework structure of $Ba_2MnSi_2O_7Cl$ can be viewed as made of an *anti*-ReO_3 type $(Ba_2Mn)Cl$ lattice centered on the acentric Si_2O_7 unit.[3] The structures of $Ba_6Mn_4Si_{12}O_{34}Cl_3$ and $Ba_6Fe_5Si_{11}O_{34}Cl_3$ form a composite framework made of $(M_{4+x}Si_{12-x}O_{34})^{9-}$ (M = Mn, $x = 0$; M = Fe, $x = 1$) covalent oxide and $(Ba_6Cl_3)^{9+}$ ionic chloride sublattices.[4]

In addition to silicates, a good number of salt-inclusion phosphates, arsenates, oxalates, and vanadates have also been synthesized by employing molten-salt methods at high temperatures[5−10] or a hydrothermal method at ∼150 °C.[11−13] These salt-inclusion compounds contain some extraordinary structural features. For example, the structure of $K_2Cs_3Cu_3(P_2O_7)_2Cl_3$ consists of 8- and 16-ring channels, in which the CsCl and KCl/CsCl salts reside, respectively.[5] The salt can be removed by washing at room temperature to give a microporous compound. The metathetic reaction between $CdCl_2$ and $K_2C_2O_4$ under hydrothermal conditions yields $[KCl][Cd_6(C_2O_4)_6] \cdot 2H_2O$, containing Cd_6O_{24} clusters with the Cl^-anions in the center.[11] The KCl sublattice forms an ordered 3-D rock-salt structure with a unit cell that is double

* To whom correspondence should be addressed. E-mail: liikh@cc.ncu.edu.tw.
† National Central University.
‡ Academia Sinica.

(1) Liao, C.-H.; Chang, P.-C.; Kao, H.-M.; Lii, K.-H. *Inorg. Chem.* **2005**, *44*, 9335.
(2) Schmidt, A.; Glaum, R. *Inorg. Chem.* **1997**, *36*, 4883.
(3) Mo, X.; Hwu, S.-J. *Inorg. Chem.* **2003**, *42*, 3978.
(4) Mo, X.; Ferguson, E.; Hwu, S.-J. *Inorg. Chem.* **2005**, *44*, 3121.
(5) Huang, Q.; Ulutagay, M.; Michener, P. A.; Hwu, S.-J. *J. Am. Chem. Soc.* **1999**, *121*, 10323.

10.1021/ic801007k CCC: $40.75
Published on Web 09/03/2008

in length that of the normal state phase. A salt-inclusion rare-earth chalcogenide, $NaSmGeSe_4 \cdot 0.25Na_2Se$, was also reported. The acentricity can be altered by salt inclusion.[9]

We have been interested in the exploratory synthesis of mixed octahedral−tetrahedral framework oxides and have reported a good number of new silicates of transition metals,[14a] main-group elements,[14b] lanthanides,[14c] and uranium[14d,e] by high-temperature, high-pressure hydrothermal and flux-growth reactions. During our continued exploration of salt-inclusion metal silicates via flux-growth techniques, we synthesized three isostructural salt-inclusion lanthanide silicates, $[K_9F_2][Ln_3Si_{12}O_{32}]$ (Ln = Sm, Eu, Gd). They are the first metal silicates that contain both K^+ and F^- ions in the structural channels. In this work, we describe the synthesis and crystal structures of these new compounds. The photoluminescence properties of the Eu compound have also been studied.

Experimental Section

Synthesis. Single crystals of the title compounds were grown by a flux method using a mixture of KF and MoO_3 (weight ratio 2/1), which melts at about 790 °C. For the synthesis of $[K_9F_2][Eu_3Si_{12}O_{32}]$ (denoted as **1**), a mixture of 0.666 g of KF, 0.333 g of MoO_3, 0.098 g of Eu_2O_3, and 0.102 g of SiO_2 in the molar ratio K/Eu/Si = 20.7:1:3 was placed in a 4-mL platinum crucible, heated to 950 °C, and isothermed for 10 h, followed by slow cooling to 870 at 2 °C/h, and then it was furnace cooled to room temperature. The flux was dissolved with hot water, and 0.177 g of colorless pillar crystals was obtained by suction filtration. A qualitative energy-dispersive X-ray analysis of several crystals confirmed the presence of K, Eu, Si, and F. Electron probe microanalysis on a crystal of **1** showed that the molar ratio was F/Eu/Si = 0.72:1:4.13, which is close to the expected ratio of 0.67:1:4. The bulk product was a single phase, as indicated by powder X-ray diffraction (Figure S1 in Supporting Information). The yield was 74% based on SiO_2.

Colorless pillar crystals of $[K_9F_2][Sm_3Si_{12}O_{32}]$ (denoted as **2**) and $[K_9F_2][Gd_3Si_{12}O_{32}]$ (denoted as **3**) were obtained by introducing a mixture of Sm_2O_3 (or Gd_2O_3) and SiO_2 in the same molar ratio as that for **1** into the KF-MoO_3 flux. The reaction mixtures were heated to 900 °C and isothermed for 10 h, followed by slow cooling to 750 at 2 °C/h, and then they were furnace cooled to room temperature. The bulk products were monophasic according to powder X-ray diffraction (Figure S1 in Supporting Information). The yields of **2** and **3** were 74% and 78%, respectively, based on SiO_2. A suitable crystal of **3** for single-crystal X-ray diffraction analysis has not been found.

Single-Crystal X-ray Diffraction. A colorless crystal of dimensions 0.03 × 0.04 × 0.3 mm for **1** and a colorless crystal of dimensions 0.02 × 0.04 × 0.23 mm for **2** were selected for indexing and intensity data collection at room temperature on a Siemens Smart CCD diffractometer equipped with a normal focus, 3-kW sealed-tube X-ray source. Empirical absorption corrections based on symmetry equivalents were performed by using the SADABS program for the Siemens area detector ($T_{min/max}$ = 0.683/0.954 for **1** and 0.746/0.945 for **2**).[15] On the basis of statistical analysis of the intensity distributions and successful solution and refinement of the structures, the space groups were determined to be $P\bar{1}$ (No. 2) for both compounds. The structures were solved by direct methods and difference-Fourier syntheses. Eu(1) (or Sm(1)) and K(4) are at inversion centers, and the other atoms are in general positions. The K and F atoms sites in the structural tunnels are ordered and fully occupied. The final cycles of least-squares refinement including the atomic coordinates and anisotropic thermal parameters of all atoms converged at R1 = 0.0217, wR2 = 0.0482, S = 1.082, and $\Delta\rho_{max,\ min}$ = 0.97, −1.19 e Å^{-3} for **1** and R1 = 0.024, wR2 = 0.0576, S = 1.0492, and $\Delta\rho_{max,\ min}$ = 1.19, −0.85 e·Å^{-3} for **2**. All calculations were carried out with the PC version of the SHELXTL program package.[16] Several crystals of **3** were selected and indexed on the same diffractometer. Reflection profile analysis indicated that all of them were twinned, and therefore, their intensity data were not collected. The unit cell parameters for **3** are a = 6.8874(6) Å, b = 11.379(1) Å, c = 11.474(1) Å, α = 87.768(5)°, β = 89.559(4)°, γ = 80.263(4)°, and V = 885.6(1) Å^3. The steady decrease in cell volume with increasing atomic number of the metal is because of lanthanide contraction.

Photoluminescence Measurements. Several crystals of **1** were contained in a glass capillary for luminescence study. A laser beam at 532 or 473 nm, which correspond to the Eu^{3+} excitation to the $^5D_1$ or $^5D_2$ state, respectively, was employed as the light source to lit up the sample for recording the emission spectra. The emission was collected by an *f*/1 focal lens and imaged onto a monochromator (Acton Research Corporation SP2300i) attached with a photomultiplier tube (PMT, Hamamatsu R636−10). To reduce the interference of laser light scattering, a Notch filter was inserted in front of the monochromator. This setup was also used for the measurements of emission radiative lifetime except the light source were replaced by a pulsed Nd:YAG laser (Spectra Physics INDI-40-10) beam at 532 nm.

Results and Discussion

Structure. The crystallographic data are given in Table 1, and selected bond lengths are given in Table 2. The three compounds are isostructural; therefore, only the structure of **1** is discussed. The asymmetric units are shown in Figure 1. The structure is constructed from the following building units: 5 K^+ cations, 1 F^- anion, 2 EuO_6 octahedra, and 6 SiO_4 tetrahedra. All atoms are in general positions, except for K(4) and Eu(1), which are at inversion centers. The observed Si−O bond lengths and O−Si−O bond angles are

(6) Huang, Q.; Hwu, S.-J.; Mo, X. *Angew. Chem., Int. Ed.* **2001**, *40*, 1690.
(7) Hwu, S.-J.; Ulutagay-Kartin, M.; Clayhold, J. A.; Mackay, R.; Wardojo, T. A.; O'Connor, C. J.; Krawiec, M. *J. Am. Chem. Soc.* **2002**, *124*, 12404.
(8) Huang, Q.; Hwu, S.-J. *Inorg. Chem.* **2003**, *42*, 655.
(9) Choudhury, A.; Dorhout, P. K. *Inorg. Chem.* **2006**, *45*, 5245.
(10) Queen, W. L.; West, J. P.; Hwu, S.-J.; VanDerveer, D. G.; Zarzyczny, M.; Pavlick, R. A. *Angew. Chem., Int. Ed.* **2008**, *47*, 1.
(11) Vaidhyanathan, R.; Neeraj, S.; Prasad, P. A.; Natarajan, S.; Rao, C. N. R. *Angew. Chem., Int. Ed.* **2000**, *39*, 3470.
(12) Vaidhyanathan, R.; Natarajan, S.; Rao, C. N. R. *J. Solid State Chem.* **2002**, *167*, 274.
(13) Vaidhyanathan, R.; Natarajan, S.; Rao, C. N. R. *Mater. Res. Bull.* **2003**, *38*, 477.
(14) (a) Kao, H.-M.; Lii, K.-H. *Inorg. Chem.* **2002**, *41*, 5644. (b) Hung, L.-I.; Wang, S.-L.; Kao, H.-M.; Lii, K.-H. *Inorg. Chem.* **2007**, *46*, 3301. (c) Lee, C.-S.; Liao, Y.-C.; Hsu, J.-T.; Wang, S.-L.; Lii, K.-H. *Inorg. Chem.* **2008**, *47*, 1910. (d) Chen, C.-S.; Lee, S.-F.; Lii, K.-H. *J. Am. Chem. Soc.* **2005**, *127*, 12208. (e) Lin, C.-H.; Chen, C.-S.; Shiryaev, A. A.; Zubavichus, Ya. V.; Lii, K.-H. *Inorg. Chem.* **2008**, *47*, 4445.
(15) Sheldrick, G. M. *SADABS, Program for Siemens Area Detector Absorption Corrections*, University of Göttingen: Göttingen, Germany, 1997.
(16) Sheldrick, G. M. *SHELXTL Programs, version 5.1*; Bruker AXS GmbH: Karlsruhe, Germany, 1998.

Table 1. Crystallographic Data for $[K_9F_2][Eu_3Si_{12}O_{32}]$ (**1**) and $[K_9F_2][Sm_3Si_{12}O_{32}]$ (**2**)

	1	**2**
chemical formula	$F_2K_9O_{32}Eu_3Si_{12}$	$F_2K_9O_{32}Sm_3Si_{12}$
a (Å)	6.8979(2)	6.9152(6)
b (Å)	11.3798(4)	11.400(1)
c (Å)	11.4964(4)	11.531(1)
α (deg)	87.607(2)	87.610(1)
β (deg)	89.470(2)	89.445(1)
γ (deg)	80.164(2)	80.081(1)
V (Å^3)	888.39(5)	894.6(1)
Z	1	1
fw	1694.86	1690.03
space group	$P\bar{1}$ (No. 2)	$P\bar{1}$ (No. 2)
T (°C)	23	21
λ(Mo Kα) (Å)	0.71073	0.71073
D_{calc} (g·cm^{-3})	3.168	3.137
∞(Mo Kα (cm^{-1})	68.1	64.3
R1[a]	0.0251	0.0240
wR2[b]	0.0633	0.0576

[a] $R_1 = [\Sigma||F_o| - |F_c||/\Sigma|F_o|$. [b] wR2 $=[\Sigma w(F_o^2 - F_c^2)^2]^{1/2}$, $w = 1/[\sigma^2(F_o^2) + (aP)^2 + bP]$, $P = [\max(F_o^2,0) + 2(F_c)^2]/3$, where $a = 0.0229$ and $b = 3.75$ for **1** and $a = 0.025$ and $b = 2.19$ for **2**.

Table 2. Selected Bond Lengths (Å) for $[K_9F_2][Eu_3Si_{12}O_{32}]$ (**1**) and $[K_9F_2][Sm_3Si_{12}O_{32}]$ (**2**)

		1	
Eu(1)−O(4)	2.296(3) (2×)	Eu(1)−O(5)	2.300(3) (2×)
Eu(1)−O(9)	2.313(3) (2×)	Eu(2)−O(1)	2.391(3)
Eu(2)−O(1)	2.354(3)	Eu(2)−O(12)	2.323(3)
Eu(2)−O(13)	2.262(3)	Eu(2)−O(14)	2.262(3)
Eu(2)−O(16)	2.349(3)	Si(1)−O(1)	1.608(3)
Si(1)−O(2)	1.669(3)	Si(1)−O(3)	1.637(3)
Si(1)−O(4)	1.589(3)	Si(2)−O(2)	1.637(3)
Si(2)−O(5)	1.571(3)	Si(2)−O(6)	1.635(3)
Si(2)−O(7)	1.633(3)	Si(3)−O(3)	1.622(3)
Si(3)−O(7)	1.629(3)	Si(3)−O(8)	1.630(3)
Si(3)−O(9)	1.574(3)	Si(4)−O(8)	1.633(3)
Si(4)−O(10)	1.634(3)	Si(4)−O(11)	1.608(3)
Si(4)−O(12)	1.582(3)	Si(5)−O(10)	1.656(3)
Si(5)−O(13)	1.596(3)	Si(5)−O(14)	1.591(3)
Si(5)−O(15)	1.660(3)	Si(6)−O(6)	1.624(3)
Si(6)−O(11)	1.607(3)	Si(6)−O(15)	1.644(3)
Si(6)−O(16)	1.580(3)	F(1)−K(1)	2.582(3)
F(1)−K(2)	2.617(3)	F(1)−K(3)	2.555(3)
F(1)−K(4)	2.705(3)		
		2	
Sm(1)−O(4)	2.315(2) (2×)	Sm(1)−O(5)	2.317(2) (2×)
Sm(1)−O(9)	2.325(3) (2×)	Sm(2)−O(1)	2.365(2)
Sm(2)−O(1)	2.406(2)	Sm(2)−O(12)	2.333(2)
Sm(2)−O(13)	2.277(3)	Sm(2)−O(14)	2.272(3)
Sm(2)−O(16)	2.360(3)	Si(1)−O(1)	1.612(2)
Si(1)−O(2)	1.671(3)	Si(1)−O(3)	1.640(3)
Si(1)−O(4)	1.584(3)	Si(2)−O(2)	1.643(3)
Si(2)−O(5)	1.572(3)	Si(2)−O(6)	1.636(3)
Si(2)−O(7)	1.636(3)	Si(3)−O(3)	1.621(3)
Si(3)−O(7)	1.630(3)	Si(3)−O(8)	1.633(3)
Si(3)−O(9)	1.579(3)	Si(4)−O(8)	1.637(3)
Si(4)−O(10)	1.640(3)	Si(4)−O(11)	1.607(3)
Si(4)−O(12)	1.587(3)	Si(5)−O(10)	1.655(3)
Si(5)−O(13)	1.596(3)	Si(5)−O(14)	1.596(3)
Si(5)−O(15)	1.663(3)	Si(6)−O(6)	1.625(3)
Si(6)−O(11)	1.608(3)	Si(6)−O(15)	1.641(3)
Si(6)−O(16)	1.583(3)	F(1)−K(1)	2.590(3)
F(1)−K(2)	2.618(3)	F(1)−K(3)	2.560(3)
F(1)−K(4)	2.713(3)		

typical values and are within the normal range.[17] The Si−O_{br} bonds between silicon and an oxygen atom O_{br} linking two Si atoms are generally longer than the Si−O_{term} bonds

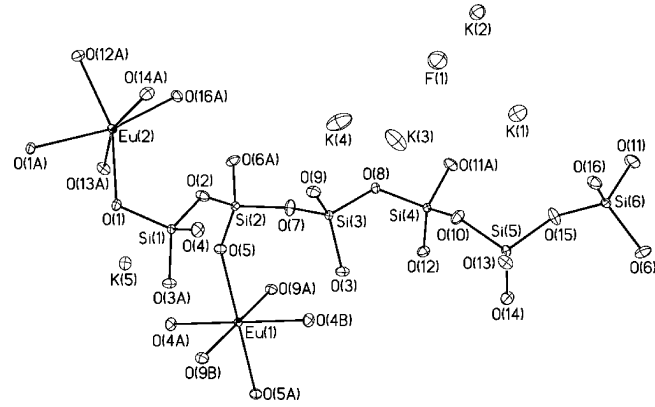

Figure 1. Building units of **1** showing the atom labeling scheme. Thermal ellipsoids are shown at 50% probability.

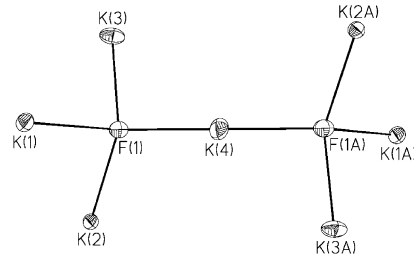

Figure 2. Coordination environments of the F atom and the K atom in **1**.

between silicon and a terminal oxygen atom O_{term} linked to only one silicon atom. $Eu(1)O_6$ is discrete and is quite regular with the Eu−O bond lengths in the range from 2.301 to 2.312 Å. $Eu(2)O_6$ shares an edge with another $Eu(2)O_6$ and is distorted with the Eu−O bond lengths ranging from 2.264 to 2.393 Å. The bond-valence sums for Eu(1) and Eu(2) are 3.2 and 3.1, respectively, indicating that all Eu atom are trivalent.[18] Each $Eu(1)O_6$ octahedron shares its six corners with six different SiO_4 tetrahedra. Each $Eu(2)_2O_{10}$ octahedral dimer shares corners with ten different SiO_4 tetrahedra. All K and F sites are fully occupied. The U_{ij} (atom displacement factor) values for the K and F atoms are normal and regular, indicating that they are not loosely bound in the structure. The coordination environment of the F atom is shown in Figure 2. The F atom is bonded to four K atoms and two FK_4 tetrahedra share a common vertex to form an F_2K_7 unit, whose structure is known among oxides such as Cl_2O_7 and Mn_2O_7 and among several anions, for example, $S_2O_7^{2-}$, $Cr_2O_7^{2-}$, $P_2O_7^{4-}$, and $Si_2O_7^{6-}$. However, the bond angle at the bridging atom, K(4), in F_2K_7 is 180°. It should be noted that the K atoms are also bound to framework O atoms. On the basis of the maximum cation−anion distance by Donnay and Allmann,[19] a limit of 3.35 Å was set for K−O interactions, which gives the following coordination numbers: K(1), 7-coordinate, including one F atom at 2.582 Å; K(2), 7-coordinate, including one F atom at 2.613 Å; K(3), 5-coordinate, including one F atom at 2.559 Å; K(4), 6-coordinate, including two F atoms at 2.706 Å; K(5), 7-coordinate and bonded to oxygen atoms only.

The SiO_4 tetrahedra are connected together by sharing

(17) Liebau, F. *Structural Chemistry of Silicates: Structure, Bonding and Classification*; Springer-Verlag: Berlin, 1985.

(18) Brown, I. D.; Altermatt, D. *Acta Crystallogr.* **1985**, *B41*, 244.

(19) Donnay, G.; Allmann, R. *Am. Mineral.* **1970**, *55*, 1003.

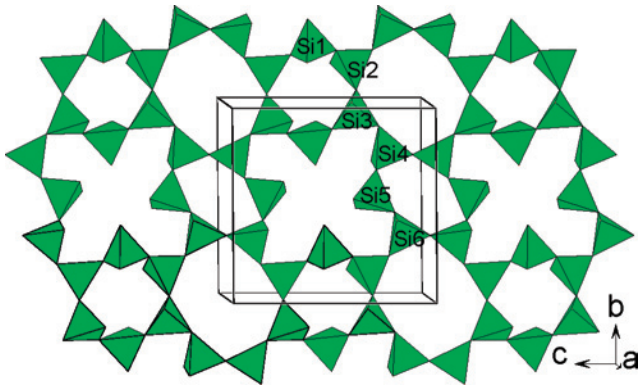

Figure 3. Silicate layer of **1** viewed along the *a*-axis to show the connectivity between adjacent loop-branched fünfer double chains.

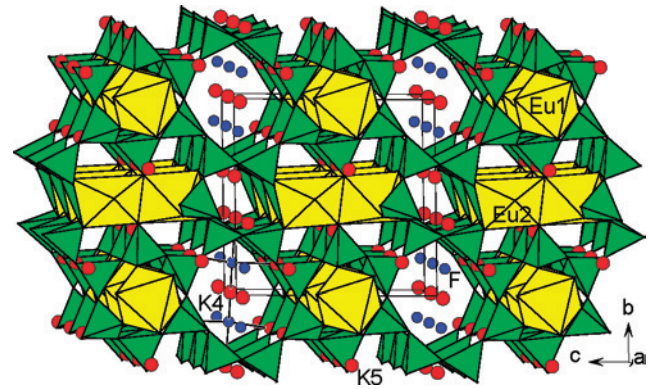

Figure 4. Structure of **1** viewed along the *a*-axis. The yellow and green polyhedra represent EuO_6 octahedra and SiO_4 tetrahedra, respectively. Red circles: K atoms. Blue circles: F atoms.

corners to form a silicate single layer in the (110) plane with the composition $[Si_6O_{16}]$ containing 6-, 8-, and 12-rings (Figure 3). According to the definition of layer types based on the periodicity of the fundamental chain from which the layer can be generated by successive linking of these chains, the layer in **1** is open-branched fünfer single layer.[17] The same type of layer has been found in synthetic $K_8Yb_3[Si_6O_{16}]_2(OH)$.[20] The composition of a silicate layer is determined by the connectedness *s* of the tetrahedra in the layer and the ratio between different types of Q^s groups. The symbols $Q^s = Q^0$, Q^1, Q^2, Q^3, and Q^4 are used to denote the tetrahedra that share zero to four corners with others. Almost all the known single layers are composed only of tertiary $[SiO_4]$ tetrahedra with the formula $[Si_{2n}O_{5n}]^{2n-}$. The layer in **1** is composed of secondary and tertiary $[SiO_4]$ tetrahedra in the ratio of 1:2, resulting in a Si/O ratio of 2:5.3. The Si/O ratio of a single layer containing more than one type of $[SiO_4]$ tetrahedra can vary considerably. For example, the single layer of synthetic $Rb_6(InCo)_2[Si_9O_{26}]$ is composed of secondary and tertiary $[SiO_4]$ tetrahedra in the ratio of 7:2, while that of synthetic $K_2[Si_4O_9]$ is composed of tertiary and quaternary $[SiO_4]$ tetrahedra in the ratio of 1:1.[21,22] Adjacent silicate layers of **1** are connected by $Eu(1)O_6$ octahedra and $Eu(2)_2O_{10}$ octahedral dimers via corner sharing to form a 3-D framework with 6-ring and 8-ring channels parallel to the *a* axis (Figure 4). The F_2K_7 units are centered at the 8-ring channels. K(5) is located at sites between adjacent silicate layers and is bonded to oxygen atoms only.

Comparison with $K_8Nd_3Si_{12}O_{32}(OH)$ and $K_{8-x}Yb_3Si_{12}O_{32}(OH)_{1-x}(H_2O)_x$. Haile et al. reported the crystal structure and ionic conductivity of hydrothermally grown crystals of $K_8Nd_3Si_{12}O_{32}(OH)$,[23] which contains $Si_{12}O_{32}$ layers almost identical to those determined here for **1**, and the neodymia-silica framework of the former is virtually identical to the europia-silica framework of the latter. The primary differences in the two structures concern the distribution of the ionic species within the 8-ring channels. In the Nd compound, rather than a K^+ cation and two F^- anions, a hydroxyl anion with an occupancy of 0.5 was found to reside close to the center of symmetry at 0.5, 0, 0.5. Thus, Haile et al. assigned their compound the stoichiometry $K_8Nd_3Si_{12}O_{32}(OH)$. The hydroxyl group is disordered because the 8-ring channel is quite large, with an average O−O distance across its diameter of 6.50 Å, which is more than twice the "diameter" of a hydroxyl group. In $K_{8-x}Yb_3Si_{12}O_{32}(OH)_{1-x}(H_2O)_x$, which was reported by Pushcharovskii et al.,[20] rather than a hydroxyl anion, a K^+ cation with $^1/_3$ occupancy was placed in the center of the eight-membered ring. The occupancy factors of another K^+ caion and an oxygen atom were refined and finally set at $^1/_2$. To balance charge, the oxygen atom was taken to represent a random distribution of hydroxyl ions and water molecules at a 1:2 atomic ratio.

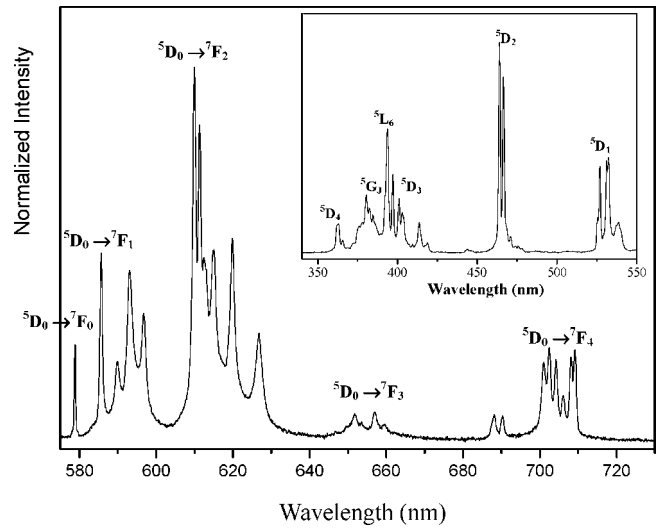

Figure 5. Room-temperature emission of **1** excited at 532 nm. The inset shows the excitation spectrum detected within the $^7F_1$ manifold (594 nm).

Photoluminescence Studies. Figure 5 shows the room-temperature (RT) emission spectrum of $[K_9F_2][Eu_3Si_{12}O_{32}]$. The RT excitation spectrum from 350 to 550 nm is shown in the inset of Figure 5. The excitation lines are assigned to the Eu^{3+} intra-$4f^6$ transitions including the $^5D_{1-4} \leftarrow {}^7F_0$, $^5L_6 \leftarrow {}^7F_0$, and $^5G_J \leftarrow {}^7F_0$ transitions. The RT emission spectrum

(20) Pushcharovskii, D. Yu.; Dago, A. M.; Pobedimskaya, E. A.; Belov, N. V. *Sov. Phys. Dokl. (Engl. Transl.)* **1981**, *26*, 552.
(21) Hung, L.-I.; Wang, S.-L.; Chen, Y.-H.; Lii, K.-H. *Inorg. Chem.* **2006**, *45*, 2100.
(22) Schweinsberg, H.; Liebau, F. *Acta Crystallogr.* **1974**, *B30*, 2202.
(23) Haile, S. M.; Wuensch, B. J.; Siegrist, T. *J. Solid State Chem.* **1999**, *148*, 406.

recorded at 532 nm excitation exhibits a number of lines between 575 and 730 nm. These lines are ascribed to emission from the first excited $^5D_0$ state to the $^7F_{0-4}$ Stark levels of the fundamental Eu^{3+} septet. The $^5D_0 \rightarrow {}^7F_0$ transition acquires its intensity via an electric-dipole transition mechanism because of the lack of an inversion symmetry center. There are two crystallographically different Eu^{3+} ions in the structure of **1**, but only one $^5D_0 \rightarrow {}^7F_0$ transition was clearly observed in Figure 5. Previously we reported a new europium silicate, $Cs_3EuSi_6O_{15}$, which contains an octahedral Eu^{3+} ion in a general position with the Eu−O bond lengths in the range from 2.266 to 2.337 Å,[14] and a very weak sharp peak was observed for its $^5D_0 \rightarrow {}^7F_0$. The $Eu(1)^{3+}$ of **1** is on a centrosymmetric site and the $Eu(1)O_6$ octahedron is quite regular with an even narrower range of Eu(1)−O bond lengths (2.302−2.312 Å) than that of $Cs_3EuSi_6O_{15}$, and therefore the $^5D_0 \rightarrow {}^7F_0$ transition of $Eu(1)^{3+}$ could be too weak to observe. This is consistent with the octahedral distortions of these sites, which can be estimated by using the equation $\Delta = (^1/_6)\Sigma[(R_i - R_{av})/R_{av}]^2$, where R_i = individual bond lengths and R_{av} = average bond length ($10^4 \times \Delta = 1.6$ and 0.05 for the Eu^{3+} in $Cs_3EuSi_6O_{15}$ and $Eu(1)^{3+}$ in compound **1**, respectively).[24] The emission spectrum originating from the higher electronic state $^5D_2$ at 473 nm excitation was also recorded, and is very similar to Figure 5 because of a very fast nonradiative relaxation except that a very weak additional peak was found in the $^5D_0 \rightarrow {}^7F_0$ transition region. This addition weak peak may correspond to the $^5D_0 \rightarrow {}^7F_0$ transition of $Eu(1)^{3+}$. In fact, the change detected on the $^5D_0 \rightarrow {}^7F_0$ transition as the excitation wavelength varies from 532 to 473 nm clearly suggests the presence of two profoundly different Eu^{3+} sites.[25]

The $^5D_0 \rightarrow {}^7F_1$ transition is magnetic-dipole allowed and relatively insensitive to coordination environment. The $^5D_0 \rightarrow {}^7F_2$ is an electric dipole transition in origin; it is absent if the ion is on an inversion center, and its intensity is very sensitive to environment. The relative intensities of the $^5D_0 \rightarrow {}^7F_1$ and $^5D_0 \rightarrow {}^7F_2$ transitions are very sensitive to the detailed nature of the ligand environment, reflecting the hypersensitive character of the $^5D_0 \rightarrow {}^7F_2$ transition. As shown in Figure 5, the integrated intensity of the $^5D_0 \rightarrow {}^7F_2$ transitions is considerably larger than that of the $^5D_0 \rightarrow {}^7F_1$ transitions. These results confirm the crystallographic data; the $Eu(2)O_6$ octahedron lacks inversion symmetry and is strongly distorted because it shares an edge with another $Eu(2)O_6$ octahedron. Moreover, compound **1** shows a slightly shorter emission lifetime ($^5D_0 \rightarrow {}^7F_2$) of approximately 3.2 ms in comparison with the value (5.45 ms) in $Cs_3EuSi_6O_{15}$. The shorter emission lifetime implies a larger electronic transition dipole moment in **1**, and this is supported by the observation that the emission intensities in **1** are brighter than those in $Cs_3EuSi_6O_{15}$.

In conclusion, the synthesis and crystal structures of three new lanthanide silicates have been reported. To our knowledge, they are the first examples of salt-inclusion compounds in lanthanide silicate systems. Several lanthanide silicate minerals, such as $Na_2MgGd_2(Si_4O_{12})F_2$ and $NaCa_2LuSi_2O_7F_2$, and a synthetic Eu silicate, $KEu_2(Si_4O_{10})F$, containing both alkali metal and F^- ions were reported.[26−28] In contrast to the title compounds which contain both K^+ and F^- ions in the structural channels, the F^- anions in these compounds are bonded to the lanthanide metals. This work makes an important addition to the structural chemistry of lanthanide silicates. The crystal structures of the title compounds consist of loop-branched fünfer double chains of silicate connected via LnO_6 octahedra to form a 3-D framework with 8-ring channels where the K^+ and F^- ions are located. The structure is closely related to those of $K_8Nd_3Si_{12}O_{32}(OH)$ and $K_{8-x}Yb_3Si_{12}O_{32}(OH)_{1-x}(H_2O)_x$, which were synthesized under hydrothermal conditions. The luminescence properties of the Eu compound have also been studied. The conclusions drawn from the relative intensities of $^5D_0 \rightarrow {}^7F_1$ and $^5D_0 \rightarrow {}^7F_2$ transitions are consistent with the crystallographic results. Although the reaction mechanism for the flux synthesis of salt-inclusion solids is unclear, one can imagine that the reactants are first dissolved in the molten salt, and then, upon cooling, the covalent lattice aggregates around the inherent structure of the molten ionic salt to form the resulting frameworks.[10,29] Therefore, it will be interesting to see whether the inclusion of other metal ions in the molten salt can direct the formation of novel silicate phases. Further research on this theme is in progress.

Acknowledgment. We thank the National Science Council of Taiwan for financial support and Prof. Sue-Lein Wang at National Tsing Hua University for X-ray data collection.

Supporting Information Available: Crystallographic data for **1** and **2** in CIF format and X-ray powder patterns. This material is available free of charge via the Internet at http://pubs.acs.org.

IC801007K

(24) Shannon, R. D. *Acta Crystallogr.* **1976**, *A32*, 751.
(25) Ananias, D.; Ferreira, A.; Rocha, J.; Ferreira, P.; Rainho, J. P.; Morais, C.; Carlos, L. D. *J. Am. Chem. Soc.* **2001**, *123*, 5735.
(26) Maisonneuve, V.; le Blanc, M. *Can. Mineral.* **1998**, *36*, 1039.
(27) Fleet, M. E.; Pan, Y.-M. *Can. Mineral.* **1995**, *33*, 879.
(28) Jacobsen, H.; Meyer, G. *Z. Kristallogr.* **1994**, *209*, 348.
(29) La Violette, R. A.; Budzien, J. L.; Stillinger, F. H. *J. Chem. Phys.* **2000**, *112*, 8072.